Azo-Azulene Derivatives as Second-Order Nonlinear Optical Chromophores

Pascal G. Lacroix,*[a] Isabelle Malfant,[a] Gabriel Iftime,*[b] Alexandru C. Razus,[b] Keitaro Nakatani,[c] and Jacques A. Delaire[c]

Abstract: The molecular and solid state nonlinear optical (NLO) properties of several (phenylazo)-azulenes are investigated. In particular, (4-nitrophenylazo)-azulene (**2b**) exhibits a quadratic hyperpolarizability (β_{vec}) of 80×10^{-30} cm^5 esu recorded at 1.907 μm by the electric field-induced second-harmonic (EFISH) technique. This molecular material, which crystallizes in the monoclinic noncentrosymmetric space group *Pc*, exhibits an efficiency 420 times that of urea in second-harmonic generation. The origin of the optical nonlinearity in azo-azulene is discussed in relation with crystal structures and semiempirical calculations within the INDO/SOS formalism, and compared with that of the well known disperse red one (DR1) organic dye.

Keywords: chromophores · donor–acceptor systems · nonlinear optics · semiempirical calculations · solvatochromism

Introduction

The elaboration of nonlinear optical (NLO) materials has attracted considerable interest for the past two decades because of their potential applications in optoelectronics, telecommunications, and optical information processing. In particular, donor–acceptor substituted π-conjugated organics with low-lying charge transfer excited states have received much attention for their large second-order NLO response.[1, 2] Many of them have been investigated both theoretically,[3, 4] and experimentally,[5] in the substituted stilbene series, which has been the most promicing family until the mid nineties. However, several new organic derivatives have recently appeared as very promicing alternative structures. Among recent examples, thiophene-based stilbene analogues have been reported to possess significantly enhanced optical nonlinearities,[2a, 6] and push–pull arylethynyl porphyrins,[7] and polyenes[8] leading to very large hyperpolarizabilities have also been under investigations. These examples illustrate the fact that the search for new NLO chromophores is still a very active research area, which now encompasses newer generations of molecules, with electronic properties of greater complexity than those of the substituted benzene previously investigated.

For instance, azulene (**1**) is a non-benzenoid aromatic molecule with a polar resonance structure (Scheme 1). One of its characteristic features is the electron drift from the seven-membered ring toward the five-membered ring. This is in accordance with an experimental dipole moment of about 0.8 D.[9] The five- and seven-membered rings of azulene carry negative and positive charges, respectively. Therefore, the five-membered ring can act as electron donor, and the seven-membered ring as electron acceptor. Owing to this property, azulene appears to be a versatile fragment which might be used for the design of various NLO materials.

1 **1'**

Scheme 1.

Several types of push–pull compounds can be imagined, in which azulene will act as donor, as acceptor or as conjugated bridge. The electron-acceptor character of azulene is supported by the reaction with nucleophiles (at the seven-membered ring),[10] or more recently by the use of an azulene derivative as acceptor in charge-transfer complexes.[11] The electron-donor character of azulene has been proven by the reaction with electrophiles (at the five-membered ring),[10] by the synthesis of charge-transfer complexes in which the azulene

[a] Dr. P. G. Lacroix, Dr. I. Malfant
Laboratoire de Chimie de Coordination (CNRS)
205 route de Narbonne
31077 Toulouse cedex (France)
E-mail: pascal@lcc-toulouse.fr

[b] Dr. G. Iftime, Dr. A. C. Razus
C.D. Nentzescu Institute of Organic Chemistry
POX 258, 71141
Bucharest 15 (Romania)

[c] Dr. K. Nakatani, Prof. Dr. J. A. Delaire
P.P.S.M. Ecole Normale Supérieure de Cachan (UMR 8531)
Avenue du Président Wilson
94235 Cachan cedex (France)

 © WILEY-VCH Verlag GmbH, D-69451 Weinheim, 2000 0947-6539/00/0614-2599 $ 17.50+.50/0

moiety acts as donor,[12] or by the stabilization of methylcations.[13] Semiempirical and ab initio calculations have shown that azulene derivatives should exhibit NLO response comparable to those of paranitroaniline, and therefore should deserve more investigations in materials chemistry.[14]

Surprisingly, only few reports on azulene-based materials with NLO properties have been published to date. The first one in 1996 by Asato et al. described compounds which contain azulene or guiazulene as electron donor groups and dicyanovinyl or 1,3-diethyl-2-thiobarbituric acid as electron-acceptor groups.[15] In the second one, we have recently reported on the first observation of second harmonic generation (SHG) in microcrystalline samples of azulene-based chromophores.[16] In particular, we found that 6-methoxy-1-[2-(4-nitrophenyl)ethenyl]-azulene exhibits an efficiency 58 times that of urea in second-harmonic generation. Recently, a ferrocene derivative connected by an ethenyl bond to the seven-membered ring of azulene was described.[17] This compound exhibits a first-order hyperpolarizability of 26×10^{-30} cm^5 esu^{-1}. No measurements of its efficiency in solid state have been reported.

In the present contribution, we wish to report on second-order NLO properties of azo-azulenes derivatives (**2**), a family of compounds that can readily be obtained by reaction of azulene (**1**) with the appropriate diazonium salt (Scheme 2).[18]

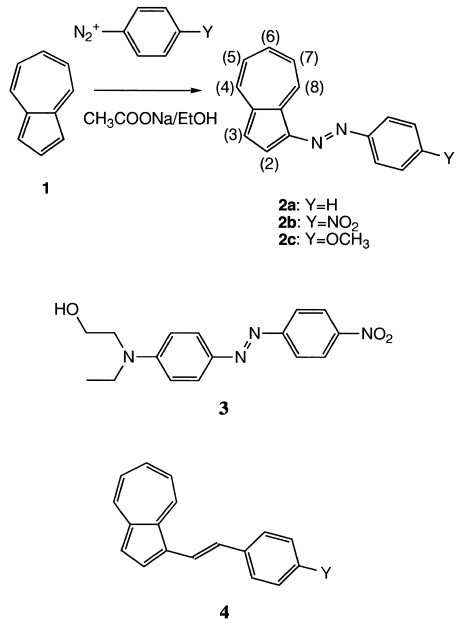

Scheme 2.

This route provides the opportunity to expand the π-conjugated system to various donor and acceptor substituents, and hence to tune the push–pull character of the chromophores. In particular, following the earlier report that azulene could have the same donating strength than *N*,*N*-diethylaniline,[15] **2b** may exhibit electronic properties related to those of 2-[*N*-ethyl-4-(4-nitrophenylazo)phenyl-amino]ethanol (DR1, **3**), which has already been widely used as NLO chromophore.[19] This possibility is supported by the resonance structures illustrated in Scheme 3. We present here an extensive study of **2b**, in comparison with **3** and with the related (phenylazo)-azulene (**2a**), and (4-methoxyphenylazo)-azulene (**2c**). The molecular hyperpolarizabilities are investigated experimentally by spectroscopy and by the electric field-induced second-harmonic (EFISH) technique,[20] in combination with a quantum chemical analysis, within the proven INDO/S-SOS formalism[4] to describe the electronic structure NLO property relationships. The relations between molecular and bulk nonlinearity are discussed in relation with the crystal structure for **2b**. Finally, the possibility to use azulene-based chromophores as radical anions is discussed.

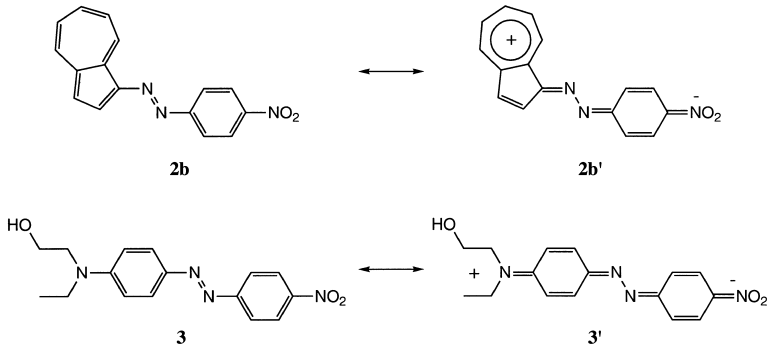

Scheme 3.

Results and Discussion

Design and general features of azo-azulenes: Contrary to 1-[2-(phenyl)ethenyl]-azulenes (**4**) derivatives, which require a 2-step synthesis in dry atmosphere and are usually obtained as a mixture of *E*:*Z* isomers,[16] 1-(4-Y-phenyl-azo)-azulenes (**2**) are readily obtained in one step, by the reaction of azulene (**1**) with the appropriate diazonium salt in ethanol, in presence of sodium acetate, at room temperature, as previously reported[18c] (Scheme 2). This route, which turns out to be suitable for linking azulene to phenyls bearing various donors and acceptors substituents, allows a modulation of the electronic properties of the chromophores. On the other hand, it is well known that the nature of the conjugation path also contributes to the extend of the NLO response.[21, 22] In particular, theoretical studies have predicted that azobenzenes should exhibit larger hyperpolarizabilities than stilbenes analogues in some cases,[21d] even if this fact is usually not observed experimentally.[5a] Therefore replacing the ethenylene fragment in **4** by azo groups might offer attracting opportunities not only from the synthetic point of view, but also for NLO purpose. It is interesting to note that, although these readily available compounds have long been known,[18a,b] before second-order NLO properties were first reported in 1961,[23]

© WILEY-VCH Verlag GmbH, D-69451 Weinheim, 2000
0947-6539/00/0614-2600 $ 17.50+.50/0 *Chem. Eur. J.* **2000**, *6*, No. 14

our study is the first NLO investigation of azo-azulene. By contrast, the related compound **3**, has been widely used for about fifteen years, especially in poled polymer matrix.[24]

Azulenic derivatives possess additional features that can attract some interest depending on the NLO applications. It is well known that second-order NLO chromophores have to be embodied into noncentrosymmetric environment if the molecular hyperpolarizability (β) has to give rise to an observable bulk susceptibility ($\chi^{(2)}$).[25] The most traditional approach which guarantees stable acentric organizations of NLO chromophores in the solid state is based on the possibility of growing large noncentrosymmetric single crystals.[26] Azulenic derivatives frequently possess low dipole moments,[14b] and it is usually assumed that they are more likely to crystallise in a non-centrosymmetric fashion, although this idea is somewhat controversial.[27] The dipole moments of the compounds investigated in the present study are gathered in Table 1. As

Table 1. Decomposition temperature (T_d in °C), redox potentials (E in V versus SCE), and dipole moments (μ in D) of azo-azulenes.

Compound (-Y)	T_d	E_{red}	E_{ox}[a]	μ[b]
2a (-H)	245	– 1.26	1.07	2.63
2b (-NO_2)	235	– 0.86	1.16	7.20
2c (-OCH_3)	275	– 1.29	0.94	2.27

[a] Peak potentials. [b] Data from ref. [28b].

anticipated, **2b** exhibits a reduced dipole than **3** (7.2 D vs 8.7 D),[28] which is indicative of possible uses of the crystal growth methodology for the design of SHG efficient material containing azulene moieties (vide infra). However, in the case of **2b** versus **3**, a difference of 1.5 D is probably not large enough to be the only reason to account for such different crystal environment.

Among other interesting physico-chemical features, azulenic derivatives frequently exhibit an excellent thermal stability,[15] which is an important prerequisite for many applications. Following this idea, the use of azulene as a donor group could give rise to thermally stable NLO chromophores. In addition, enhanced thermal stabilities of the azobenzene derivatives versus the stilbene analogues has also be reported.[29] The values given in Table 1 indicate a good range of stability for **2** (235 – 275 °C).

Description of the structures: Figures 1, 2, and 3 illustrate the atomic numbering scheme employed for molecules **2b**, **2c**, and **3**, respectively. The X-ray structure analyses of **2b** reveals two molecules present in a non centrosymmetric crystal cell (monoclinic space group *Pc*), which refer to one another by a glide mirror. The molecule is quasi planar, with a largest deviation of 0.131 Å observed at O(2). The structure of **2c** consists of four discrete molecules embodied in a centrosymmetric environement. Two molecules are present in the asymmetric unit cell (molecules 1 and 2). The angle between the mean plan of molecules 1 (largest deviation of 0.174 Å at C(15)) and 2 (largest deviation of 0.043 Å at C(33)) is equal to 80.0°. The asymmetric unit cell of **3** is made of two molecules of dye with an additionnal molecule of water. The largest deviation from planarity is 0.158 Å at O(12) for molecule 1,

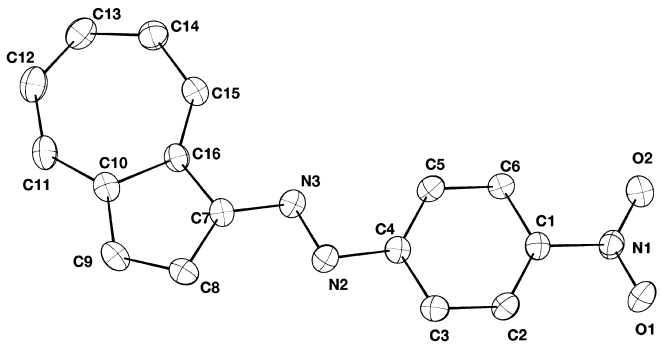

Figure 1. Atom labeling scheme, and thermal vibration ellipsoids for **2b**. H atoms are omitted for clarity.

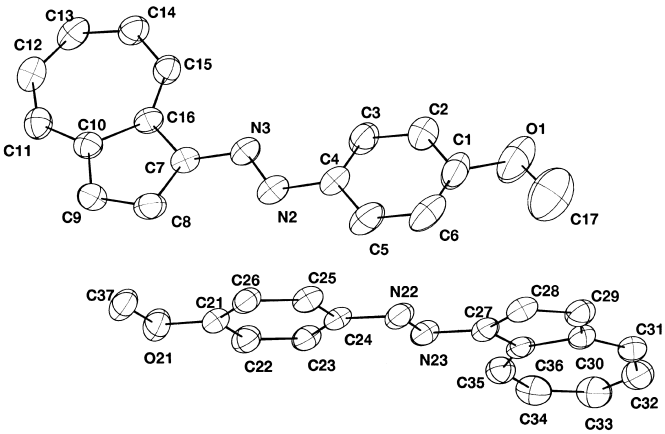

Figure 2. Atom labeling scheme, and thermal vibration ellipsoids for **2c** molecule 1 (top) and molecule 2 (bottom). H atoms are omitted for clarity.

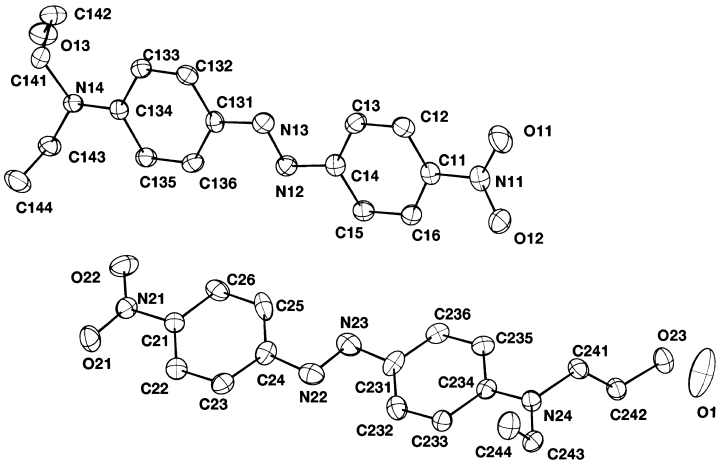

Figure 3. Atom labeling scheme, and thermal vibration ellipsoids for **3** molecule 1 (top) and molecule 2 (bottom). H atoms are omitted for clarity.

and 0.113 Å at O(21) for molecule 2. The angle between the dyes is equal to 46.5°. The majority of the azobenzene containing structures reported in the litterature show significant twist of at least one of the phenyl rings within the azobenzene frame.[30] This situation is not observed here, with angles between the phenyl and the azulene mean plans equal to 4.5°, 8.8° and 1.8° for **2b** and **2c** (molecule 1 and 2), respectively. These values are in the same range of magnitude

of the 3.1° and 5.7° measured between the two aromatic rings of **3** (molecule 1 and molecule 2, respectively). Selected bond lengths are given in Table 2. A shortening of the two C–N bond, with averages of 1.405(3), 1.407(4), 1.404(4) Å for **2b** and **2c** (molecule 1 and molecule 2), respectively, are indicative of significant conjugation of the whole π system. These bond lengths are shorter than the 1.412(3) Å and 1.438(4) Å found for **3** (molecule 1 and 2, respectively). In addition, the Table reveals an increase of the N–N bond lengths, in the azulenic derivatives versus those of **3**. All these features allow the possibility of long range electron delocalization.

Table 2. Selected bond lengths (Å) for **2b**, **2c**, and **3**.

2b	
C(4)–N(2)	1.424(3)
N(2)–N(3)	1.277(3)
N(3)–C(7)	1.387(3)
2c	
C(4)–N(2)	1.424(4)
N(2)–N(3)	1.280(3)
N(3)–C(7)	1.390(4)
C(24)–N(22)	1.419(4)
N(22)–N(23)	1.288(3)
N(23)–C(27)	1.389(4)
3	
C(14)–N(12)	1.425(3)
N(12)–N(13)	1.262(3)
N(13)–C(131)	1.400(3)
C(24)–N(22)	1.460(4)
N(22)–N(23)	1.241(3)
N(23)–C(231)	1.416(4)

Optical spectroscopy: The absorption spectra of **2b** and **3** recorded in dioxane are compared in Figure 4. Both exhibit an intense band at 460 nm ($\varepsilon = 31\,700\ \mathrm{M^{-1}\,cm^{-1}}$) and 474 nm ($\varepsilon = 31\,000\ \mathrm{M^{-1}\,cm^{-1}}$) for **2b** and **3**, respectively. The absorption

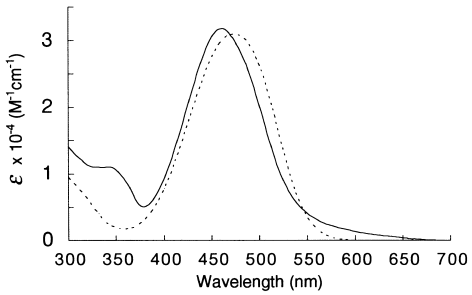

Figure 4. Electronic spectrum for **2b** recorded in dioxane, **3** (dotted line) is given as a reference.

maxima (λ_{max}) recorded in solvent of different polarities are given in Table 3. The data clearly indicate that **2b** and **3** exhibit a strong solvatochromism, with λ_{max} values lying in the same range of magnitude (450–500 nm) depending on the solvent. Solvatochromism is usually indicative of a change in dipole moments ($\Delta\mu$) upon electronic excitations. According to the well known and widely used "two-level model",[20a, 31] the hyperpolarizability (β) of "push–pull" π-organic chromophores is well described in term of a ground and an excited state having charge transfer character, and is related to the energy of the optical transition (E), its oscillator strength (f), and the difference between ground and excited state dipole moment ($\Delta\mu$) through the relation:

$$\beta = \frac{3\,e^2\,\hbar f\,\Delta\mu}{2\,m\,E^3} \times \frac{E^4}{(E^2-(2\hbar\omega)^2)(E^2-(\hbar\omega)^2)} \quad (1)$$

in which $\hbar\omega$ is the energy of the incident laser beam. Equation (1) shows that large solvatochromism is strongly indicative of a large hyperpolarizability. Solvatochromism analysis (see Experimental Section) gives $\Delta\mu$ values of 3.1 and 5.2 D for **2b** and **3**, respectively. Therefore, assuming a two-level description of the NLO response, comparable intensities, λ_{max} and solvatochromic shifts evidenced for **2b** and **3** suggest the same β magnitude for both chromophores.

Table 3. Absorption maxima (λ_{max} in nm) of the low energy charge transfer transitions for **2a–c** and **3** in solvents of different polarities.

	2a	**2b**	**2c**	**3**
cyclohexane	417	450	425	454
CCl_4	422	458	429	458
dioxane	422	460	428	474
ethyl acetate	420	462	424	480
THF	423	464	428	488
toluene	424	468	430	464
CH_2Cl_2	424	472	428	482
DMF	426	474	430	502
chloroform	424	478	429	472
MeOH	421	480	425	465
EtOH	422	482	425	465
CH_3CN	421	486	426	466
acetone	421	487	423	466
DMSO	428	506	434	483

These observations can be compared with the INDO derived spectroscopic properties gathered in Table 4. In the case of **3**, the calculation indicates a single intense absorption maxima located at 402 nm ($f = 1.24$) and 379 nm ($f = 1.12$) for molecule 1 and 2, respectively, a difference which is due to different molecular geometries. Molecule 2 is slightly twisted (5.7°) versus molecule 1 (3.1°), a situation which can reduce the overlap and hence the intensity (f) and the wavelength of the electronic transition. In the case of **2b**, two intense and closely located transitions at 445 nm (1 → 3) and 440 nm (1 → 4) can account for the experimental band observed at 460 nm. The sum of their intensity lies in the range of magnitude of that calculated for **3**, in agreement with the experimental extinction coefficients. We make the assumption that the calculated spectra (λ_{max} and intensities) roughly fit the

Table 4. Comparison of experimental (in dioxane) and INDO derived spectroscopic data (λ_{max} in nm, ε in M^{-1} cm^{-1}, oscillator strength (f) and $\Delta\mu$ in D) for **2b** and **3**.

	Experimental				INDO		
	λ_{max}	ε	$\Delta\mu$		λ_{max}	f	$\Delta\mu$
2b	460	31700	3.1	1 → 3	445	0.77	4.7
				1 → 4	440	0.45	1.7
3	474	31000	5.2	molecule 1	402	1.24	13.7
				molecule 2	379	1.12	14.7

© WILEY-VCH Verlag GmbH, D-69451 Weinheim, 2000
0947-6539/00/0614-2602 $ 17.50+.50/0 *Chem. Eur. J.* **2000**, *6*, No. 14

experimental data, in order to relate the NLO response and the INDO-based electronic properties in the next Section. However, it must be noticed that the agreement between calculated and experimental $\Delta\mu$ value is not excellent for compound **3**. Although the origin of this difference has not been carefully analysed, it has to be reminded here that experimental estimations of $\Delta\mu$ by mean of solvatochromic shifts may not be fully reliable in some cases.[32] In particular, this method implies the knowledge of the Onsager radius, a parameter hard to define for these compounds (see Experimental Section).

Molecular hyperpolarizabilities: The hyperpolarizabilities of **2a–c** were measured by the EFISH technique. In this technique, the noncentrosymmetry of the solution is induced by dipolar orientation of the chromophores by a pulse of high voltage, yielding a signal proportional to the square of Γ, the third-order nonlinear coefficient. Γ and β are related by the relation:

$$\Gamma = Nf^{2\omega}f^{\omega}f^{0}(\gamma+\mu\beta_{vec}/5kT) \quad (2)$$

N is the number of chromophore per unit volume, $f^{2\omega}$, f^{ω} and f^{0} are Lorentz local field factors. If the cubic hyperpolarizability (γ) is neglected, EFISH, combined with the measure of the dipole moment (μ) leads to β_{vec}, the vector component of the β_{ijk} tensor along the dipole moment direction. The EFISH data are gathered in Table 5. It must be reminded here from Equation (1), that β (and hence β_{vec}) are dependent on the energy of the incident laser beam. On the other hand, $(3e^2\hbar f\Delta\mu)/2mE^3$ is the static hyperpolarizability $\beta_{(0)}$, independent on the laser. This is the parameter of interest to take into account for the comparison of the intrinsic optical nonlinearity of the molecules. $\beta_{(0)vec}$ is equal to 57×10^{-30} cm^{-5} esu^{-1} for **2b**, a value close to the 47×10^{-30} cm^{-5} esu^{-1} measured for **3**. It must be observed that the agreement between experimental and INDO data is satisfactory for **2b** and **c**.

A chemical quantum analysis can provide a rationale for the understanding of the origin of the NLO response of **2b** versus that of **3**. The INDO calculated hyperpolarizabilities are reported in Table 5. The data indicates the β enhancement when the second harmonic is close to the absorption maxima, in agreement with Equation (1). It must be observed that INDO-SOS calculation indicates the same magnitude for the NLO response of both compounds, the hyperpolarizability of **2b** (43.6×10^{-30} cm^5 esu^{-1}) being slightly higher than the averaged value calculated for **3** (40.6×10^{-30} cm^5 esu^{-1}), in agreement with the experimental data. This qualitative agreement makes the analysis of the calculations reliable. Within the framework of the SOS perturbation theory, the molecular hyperpolarizability can be related to all excited states of the molecule and can be partitioned into two contributions, so called two-level (β_{2level}) and three-level (β_{3level}) terms.[33] Analysis of term contributions to the molecular hyperpolarizability of **2b** and **3** indicates that two-level terms dominate the nonlinearity. Table 6 indicates the main electronic transitions involved in β_{2level} for compounds **2** and **3**. In the case of **2b**, it can mainly be related to the dominant $1\rightarrow3$ transition, which contribute 45% to the nonlinearity, while the single $1\rightarrow5$ transition account for about 90% of the β_{2level} of **3**. Therefore, understanding these transitions provides qualitative understanding of β. The charge transfer associated with these transitions are compared in Figure 5. It clearly appear that the five-membered ring of the azulene moiety acts as the donor in **2 b**.

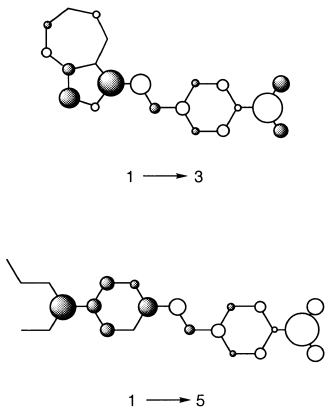

Figure 5. Differences in electronic populations between the ground state and the excited state for the main transitions involved in the NLO response of **2b** ($1\rightarrow3$ transition) and **3** ($1\rightarrow5$ transition). The white (black) contributions are indicative of an increase (decrease) of electron density in the charge transfer process.

Table 5. INDO-SOS NLO response (β_{total}, β_{2level}, and β_{vec} in 10^{-30} cm^5 esu^{-1}) at various wavelengths (incident laser beam), compared with experimental β_{vec}, and SHG powder efficiences ($I^{2\omega}$) versus that of urea for **2a–c** and **3**.

	Calculated hyperpolarizabilities									Experimental data[a]			
	$\beta_{(1.064\,\mu m)}$			$\beta_{(1.907\,\mu m)}$			$\beta_{(0)}$			β_{vec}		$\beta_{(0)vec}$	$I^{2\omega}$
	total	2 level	vec	total	2 level	vec	total	2 level	vec	1.907 μm	1.356 μm		1.907 μm
2a	36.0	26.7	2.3	17.4	16.5	13.2	16.0	14.2	→ **12.7**	7.1		→ **5.4**	6.5
2b	252.2	328.3	242.2	68.9	104.0	62.8	50.0	80.8	→ **43.6**	80		→ **57**	420
2c										< 5.4[c]		→ < **4.1**[c]	0
molecule 1	32.9	24.2	4.5	18.9	19.0	11.3	17.2	18.1	→ **10.3**				
molecule 2	33.3	29.2	4.4	21.0	26.5	14.2	18.7	22.6	→ **12.6**				
3											125[b]		
molecule 1	153.6	243.7	151.0	63.7	122.0	62.4	47.7	98.3	→ **46.6**				
molecule 2	96.2	162.7	92.9	46.1	93.6	44.7	35.8	77.9	→ **34.7**				

[a] Experimental $\beta_{(0)}$ obtaines using 2-level description, with $\beta_{(0)}=\beta[1-(2\lambda_{max}/\lambda_{\omega})^2][1-(\lambda_{max}/\lambda_{\omega})^2]$. [b] Data from ref. [27]. [c] Limited accuracy due to weak EFISH signal.

Table 6. Energies (λ_{max} in nm), oscillator strengths (f), dipole moment changes between ground and excited state ($\Delta\mu$ in D), contribution in the β_{2level}, and composition of the main two transitions involved in the NLO responses of **2** and **3**.

Compound	Transition	λ_{max}	f	$\Delta\mu$	State (%)[a]	Composition[b] of CI expansion
2a	$1\rightarrow8$	267	0.62	7.1	30	$-0.489_{\chi42\rightarrow45}+0.479_{\chi41\rightarrow44}-0.413_{\chi43\rightarrow46}$
	$1\rightarrow9$	250	0.50	7.4	21	$-0.411_{\chi41\rightarrow44}-0.408_{\chi42\rightarrow44}-0.393_{\chi42\rightarrow45}$
2b	$1\rightarrow3$	445	0.77	4.7	45	$-0.714_{\chi51\rightarrow52}-0.438_{\chi45\rightarrow52}+0.371_{\chi45\rightarrow54}$
	$1\rightarrow4$	440	0.45	1.7	9	$0.579_{\chi45\rightarrow52}-0.540_{\chi51\rightarrow52}-0.485_{\chi45\rightarrow54}$
2c						
molecule 1	$1\rightarrow4$	423	0.88	1.86	27	$-0.795_{\chi49\rightarrow50}-0.359_{\chi49\rightarrow51}$
	$1\rightarrow9$	255	0.71	10.0	26	$0.523_{\chi48\rightarrow51}-0.482_{\chi48\rightarrow50}-0.379_{\chi49\rightarrow52}$
molecule 2	$1\rightarrow9$	257	0.69	11.35	29	$-0.626_{\chi48\rightarrow51}+0.400_{\chi48\rightarrow50}+0.375_{\chi49\rightarrow52}$
	$1\rightarrow4$	430	0.82	1.55	22	$-0.806_{\chi49\rightarrow50}-0.396_{\chi45\rightarrow50}$
3						
molecule 1	$1\rightarrow5$	403	1.24	13.74	92	$0.818_{\chi60\rightarrow61}+0.477_{\chi60\rightarrow62}$
	$1\rightarrow9$	267	0.18	17.1	5	$-0.801_{\chi59\rightarrow61}-0.389_{\chi60\rightarrow61}$
molecule 2	$1\rightarrow5$	352	1.12	14.7	87	$-0.762_{\chi60\rightarrow61}-0.562_{\chi60\rightarrow62}$
	$1\rightarrow9$	262	0.22	22.5	8	$0.718_{\chi59\rightarrow60}-0.474_{\chi60\rightarrow61}$

[a] State % $=\beta_{g\rightarrow e(i)}/\Sigma_i\beta_{g\rightarrow e(i)}$. [b] Orbital 43 is the HOMO and 44 the LUMO for **2a**, orbital 51 is the HOMO and 52 is the LUMO for **2b**, orbital 49 is the HOMO and 50 the LUMO for **2c**, orbital 60 is the HOMO and 61 the LUMO for **3**.

By contrast, **2a** and **2c** are modest chromophores. Interestingly, the experimental and calculated magnitudes of β_{vec} (Table 5) significantly disagree, although it clearly appears that the NLO responses are deeply reduced versus that of **2b** and **3**. We may tentatively relate this discrepancy to the fact that the dipole moments of **2a** and **2c** are deeply reduced (Table 1) and no longer parallel to β. Large experimental uncertainties can arise from small EFISH signals (proportional to μ). This effect becomes dramatic at 1.064 μm where β and μ are almost orthogonal, which leads to almost vanishing β_{vec} (Table 5). Moreover, the modest INDO accuracy on the angle value between β and μ can affect the magnitude of β_{vec}, especially as the angle value is large. The fact that calculations are based on solid state molecular structures, whereas molecules in solution can adopt another geometry may also explain the discrepancy between theory and experiments. However, it clearly appears either from experimental or calculated data that the NLO response of **2a** and **2c** is far reduced versus that of **2b** and **3**. Although no transition clearly dominate their NLO response, as indicated in Table 6, the origin of the charge transfers (and hence β) can unambigously be found in the azulene moiety itself. This is evidenced in Figure 6, in which the directions and magnitudes of β are compared for the four chromophores. While **2b** and **3** exhibit the same features with a strong charge transfer involving the whole π-electron system, **2a** and **2c** exhibit electronic properties dominated by the azulene fragment. Consequently, such chromophores should exhibit similar and rather modest λ_{max}, solvatochromic shift (Table 3) and β (Table 5), whatever the donating strength of the phenyl substituent would be.

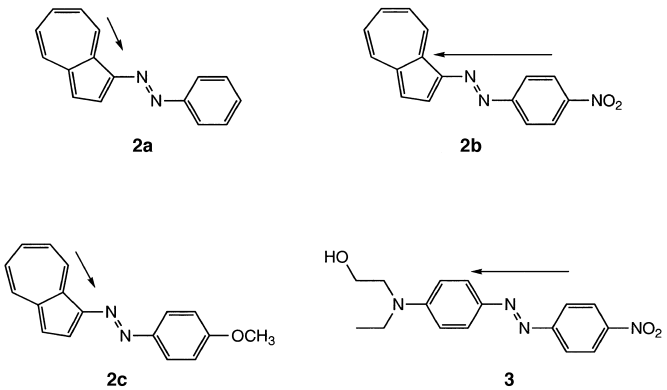

Figure 6. Orientation of β for **2a–c** and **3**.

Bulk efficiencies in second-harmonic generation: In molecular materials, the susceptibility tensor ($\chi^{(2)}$) which determines the second-order response is related to the underlying molecular hyperpolarizability tensor (β). The above section has shown that **2b** possesses a large β, in the range of magnitude of that of the well known molecular structure **3**. However, the main bottleneck to the development of molecular second-order NLO material is the compulsory noncentrosymmetric environment of the chromophores if the molecular hyperpolarizability is to contribute to an observable bulk nonlinear susceptibility.[25] It is generally assumed that traditionnal push–pull chromophores, such as 1,4-disubstituted benzene and 4,4′-disubstituted stilbene, have large dipole moments and approximately linear shapes, which cause most of them to crystallize in centrosymmetric space groups. One strategy employed to encourage noncentrosymmetric crystallization of neutral organic chromophores is to increase their geometrical asymmetry by introducing a substituent in the *ortho* or *meta* position of one of the aromatic rings. Thus, whereas crystals of 4-nitroaniline are centrosymmetric, 2-methyl-4-nitroaniline crystallize in the noncentrosymmetric space group *Cc*.[34, 35] Another strategy is to lower the ground state dipole moment, without cancelling the intramolecular charge transfer. 3-Methyl-4-nitropyridine-1-oxide was the first organic material that exemplifies with success this strategy.[36] Along these lines, it seems that the substituted azulenes investigated in the present study should offer more chance for noncentrosymmetric crystallization, by virtue of their bent shape and reduced dipole moment. However, the development of single-crystal NLO materials is hamped by the absence of general rules for predicting crystal structure from molecular structure, and the zero efficiency of **2c** (Table 5) proves the limitations of this methodology.

 © WILEY-VCH Verlag GmbH, D-69451 Weinheim, 2000 0947-6539/00/0614-2604 $ 17.50+.50/0 *Chem. Eur. J.* **2000**, *6*, No. 14

Nevertheless, the noncentrosymmetric crystal structure of **2b** allows an investigation of the relations between microscopic and macroscopic second-order optical nonlinearities for this material.

Following Zyss approach,[26] the hyperpolarizability tensor (components β_{ijk} in the molecular frame) is related to the corresponding crystalline first-order nonlinearity $\chi^{(2)}$ (components d_{IJK} in crystalline frame) through the following relation:

$$d_{IJK}(-2\omega;\omega,\omega) = N f_I^{2\omega} f_J^{\omega} f_K^{\omega} \Sigma \cos(I,i)\cos(J,j)\cos(K,k)\beta_{ijk}$$

N is the number of chromophores per unit volume, $f_I^{2\omega}$, f_J^{ω}, and f_K^{ω} are Lorentz local-field factors. The summation is performed over all molecules in the unit cell, and the cosine product terms represent the rotation from the molecular reference frame into the crystal frame. **2b** crystallizes in space group *Pc* (monoclinic point group 2). Assuming a simplified one-dimensional description of the molecular nonlinear tensor of the molecules, β has only one non vanishing coefficient along the charge transfer axis x of the molecule (namely β_{xxx}). This model leads to

$$d_{ZZZ} = N\beta_{xxx}\cos^3\theta$$

$$d_{ZXX} = N\beta_{xxx}\cos\theta\sin^2\theta$$

where the Lorentz local-field factors have been assumed equal to 1. All other components of the tensor are negligible (θ is defined as the angle between the main intramolecular charge transfer axis *0x* and the glide mirror of the crystal). The optimization of d_{ZZZ} can be achieved with $\theta = 0^\circ$, while the angular factor weighting β_{xxx} in the expression of d_{ZXX} is maximized and equal to 0.385 for $\theta = 54.74^\circ$. The orientation of β in the crystal cell is shown in Figure 7. θ reaches a value of

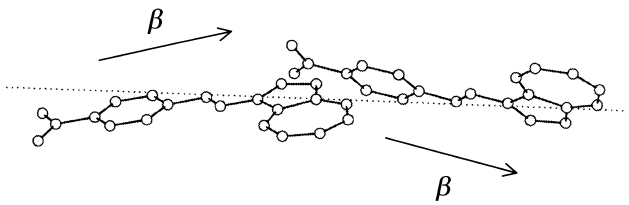

Figure 7. CAMERON view of **2b** showing the angle ($\theta = 15.1^\circ$) between β and the glide mirror (dotted line) of the cell.

15.1°, which corresponds to angular factors of 0.901 and 0.065 for d_{ZZZ} and d_{ZXX}, respectively. Assuming the calculated β value of 68.9×10^{-30} cm^5 esu^{-1} and the crystallographic determination of $N = 3.15 \times 10^{21}$ cm^{-3} lead to $d_{ZZZ} = 19.6 - 10^{-8}$ cm^2 esu^{-1} and $d_{ZXX} = 1.41 \times 10^{-8}$ cm^2 esu^{-1}. These data indicate a large quadratic NLO response for the crystal. Consequently, the SHG efficiency of **2b** has been found to be 420 times that of urea (Table 5), a very large value for this new class of materials.

Electrochemical properties of azulene-based chromophores: Beside NLO properties, azulene derivatives possess electronic features of greater complexity than those of the earliest benzene derivatives, such as the possibility of forming radical anions, which could be used in the design of organic metals.[11] In order to further understand the electrochemical properties of these molecular materials, we have drawn the frontier orbitals of **2b** and **2c** in Figure 8. Interestingly, it can be

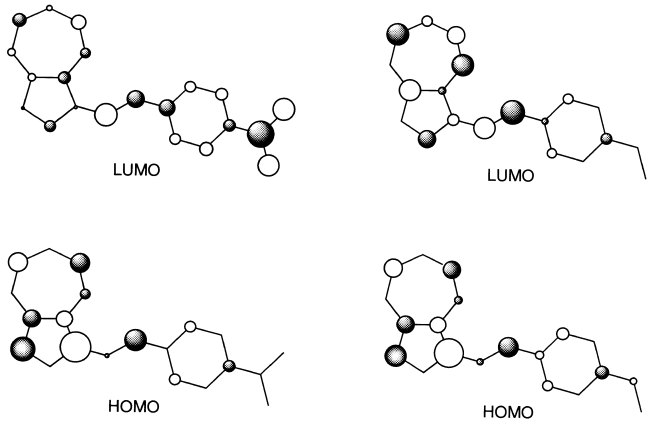

Figure 8. Comparison of the frontier orbitals for **2b** (left) and **2c** (right).

observed that most of the electron density of the highest occupied molecular orbital (HOMO) is carried by the azulene fragment, in both cases. Therefore, the HOMO of **2b** and **2c** exhibit the same features. This is consistent with oxydation potentials lying in the same range of magnitude (Table 1) whatever the nature of the substituted phenyl is. By contrast, the lowest unoccupied molecular orbitals (LUMO) of both materials are very different. In **2b**, most of the electron density is located on the nitrophenyl substituent, in relation with the withdrawing effect of NO_2. This observation results in a shift of the reduction potentials to higher values for this material (Table 1).

The possibility to isolate stable radical anions is illustrated in Figure 9 for **2b**. Two reduction processes are observed at

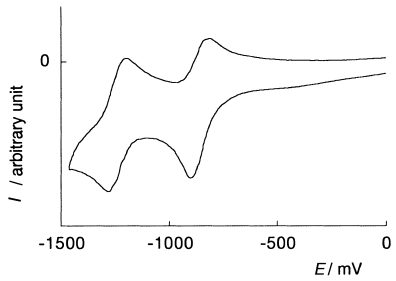

Figure 9. Cyclic voltammogram of **2b** in acetonitrile.

-0.86 V (E_1) and -1.24 V (E_2). They exhibit satisfactory reversibilities ($E_{red} - E_{ox} = 88$ mV and 71 mV for E_1 and E_2, respectively). The stability of the radical anion depends on the comproportionation constant (K_{con}), calculated for the equilibrium

$$\mathbf{2b} + (\mathbf{2b})^{2-} \overset{K_{con}}{\rightleftharpoons} 2(\mathbf{2b})^{-}$$

the redox potential being as follows: $E_1 - E_2 = 0.059 \log (K_{con})$. A potential difference of 0.38 V leads to large

comproportionation constant ($K_{con} = 2.75 \times 10^6$), which indicates that radicals such as **2b** could be isolated and characterized. Interestingly, it has recently been mentioned that radicals might offer intriguing candidates for NLO purpose.[37–39] This might stimulate further challenging researches using azulene-based radicals as NLO materials with extended electronic properties.

Conclusion

After having focused on relatively simple NLO systems with particular emphasis on the paranitroaniline family, chemists have increasingly extended the field of their investigations over the last few years. We have presented here the second-order NLO properties of azo-azulene derivatives. At the molecular level, **2b** exhibits a 57×10^{-30} cm^{5}esu^{-1} $\beta_{(0)}$ value a little higher than that of the well known "Disperse Red 1" (**3**) chromophore. Interrestingly, **2b** crystallizes in the noncentrosymmetric space group *Pc* which results in a SHG efficiency 420 times that of urea.

Over the last two decades, intense activity has demonstrated at both molecular and crystalline levels the relevance of organic media for quadratic nonlinear optics. Azulene-based materials which have received very limited attention in nonlinear optics are a family of readily available compounds, which offer additional electronic features (e.g. reversible redox properties) which could make them attracting candidates as multi-functional molecular devices.

Experimental Section

Reagents and equipment: Disperse Red 1 (**3**), azulene (**1**), and aromatic amines for coupling reactions were used as commercial samples. Basic alumina (activity B II-III, Brockmann) was used for column chromatography. TLC analysis was carried out on Merck Aluminoxid 60 F_{254} aluminum plates. The proton and carbon spectra were recorded on a Bruker AC-F 200 NMR spectrometer. Mass spectra were recorded on a SQMD 1000-Carlo Erba 5300 Mega Series mass spectrometer with capillary column, at 70 eV. Electronic spectra were recorded on a Hewlett–Packard 8452 A spectrophotometer. Thermal measurements were performed by TG/DTA analysis on a Setaram-TGDTA92 thermoanalyser. The experiments were conducted under nitrogen on 5 mg of sample (rate of heating: 10 °C per min). The decomposition temperature (T_d) was assigned as the intercept of the leading edge of the decomposition endotherm with the base line of the DTA scan.[29, 40]

Azulene-1-azobenzene (2a) and azulene-1-azo(4′-methoxybenzene) (2c): A solution of aryldiazonium chloride was prepared at 0 °C, by adding sodium nitrite (37 mg, 0.54 mmol) to a solution of aromatic amine hydrochloride (0.54 mmol) and concentrated HCl (0.9 mL) dissolved in water (2 mL). This solution was slowly added, with stirring, to a mixture of azulene (72 mg, 0.44 mmol) and sodium acetate (170 mg) in ethanol (10 mL) at room temperature. After 10 more minutes stirring, the reaction mixture was extracted with CH_2Cl_2. The organic solution was washed with 5% aqueous ammonia then with water, and dried (Na_2SO_4). The solvent was evaporated and the residue was purified by column chromatography with *n*-pentane/CH_2Cl_2 5:1 on alumina. The product (dark-brown crystals) was then crystallised from *n*-hexane.

Azulene-1-azobenzene (2a): Yield: 82 mg, 81%; m.p.: 120 °C (lit.: 120–121 °C).[18c] MS (*m/z*): 232 $[M]^+$; ^{1}H NMR (CD_2Cl_2): $\delta = 9.36$ (d, $J =$ 9.8 Hz, 1H, $H_{(8)}$), 8.39 (d, $J = 9.3$ Hz, 1H, $H_{(4)}$), 8.30 (d, $J = 4.6$ Hz, 1H, $H_{(2)}$), 7.97 (m, 2H, C_6H_5), 7.80 (t, $J = 9.8$ Hz, 1H, $H_{(6)}$), 7.54 (m, 2H, C_6H_5), 7.46 (d, $J = 4.3$ Hz, 1H, $H_{(3)}$), 7.45 (m, 2H, $H_{(5-7)}$, C_6H_5), 7.37 (t, $J = 9.7$ Hz, 1H, $H_{(5-7)}$); ^{13}C NMR ($CDCl_3$): $\delta = 154.1$, 143.9, 143.8, 139.5, 138.7, 138.5, 135.5, 129.2, 129.0, 126.5, 126.4, 125.2, 122.2, 119.9; ^{1}H NMR ($CDCl_3$) and ^{13}C NMR ($CDCl_3$) are in agreement with the ones previously reported.[41] $C_{16}H_{12}N_2$: calcd C 82.73, H 5.21, N 12.06; found C 82.65, H 5.30, N 12.05.

Azulene-1-azo-(4′-methoxybenzene) (2c): Yield: 98 mg, 84%; m.p.: 98 °C (lit.: 96 °C);[18a,b] MS (*m/z*): 262 $[M]^+$; ^{1}H NMR (CD_2Cl_2): $\delta = 9.31$ (d, $J =$ 9.8 Hz, 1H, $H_{(8)}$), 8.35 (d, $J = 9.3$ Hz, 1H, $H_{(4)}$), 8.28 (d, $J = 4.5$ Hz, 1H, $H_{(2)}$), 7.97 (d, $J = 8.9$ Hz, 2H, C_6H_4), 7.75 (t, $J = 9.9$ Hz, 1H, $H_{(6)}$), 7.44 (d, $J = 4.9$ Hz, 1H, $H_{(3)}$), 7.43 (t, $J = 9.7$ Hz, $H_{(5-7)}$), 7.32 (t, $J = 9.7$ Hz, 1H, $H_{(5-7)}$), 7.05 (d, $J = 8.9$ Hz, 2H, C_6H_4), 3.90 (s, 3H, CH_3); ^{13}C NMR ($CDCl_3$): 160.8, 148.5, 143.9, 143.5, 139.4, 138.3, 137.9, 135.5, 126.1, 125.9, 125.1, 123.8, 119.7, 114.2, 55.6; $C_{17}H_{14}N_2O$: calcd C 77.82, H 5.38, N 10.68; found C 77.77, H 5.40, N 10.61.

Azulene-1-azo-(4′-nitrobenze) (2b): 4-Nitroaniline (9 mg, 0.5 mmol) were dissolved in a mixture of concentrated H_2SO_4 (1 mL) and a drop of water. The mixture was heated for 5 min to ensure complete dissolution of the amine, then cooled at 0 °C. A solution containing sodium nitrite (35 mg, 0.5 mmol) in water (0.5 mLI was slowly added to the reaction mixture, and the solution was allowed to stand at room temperature for 5 min. The solution of the resulting diazonium salt was then slowly added under stirring to a cooled suspension (0 °C) containing azulene (64 mg, 0.5 mmol) and sodium acetate (2 g) in ethanol (5 mL. The mixture was stirred for 10 min at room temperature, then the organic compound was separated between CH_2Cl_2 and a 20% aqueous solution of sodium carbonate. The organic layer was dried (Na_2SO_4) then the solvent evaporated. The crude residue was purified by column chromatography with CH_2Cl_2 on alumina. After evaporation of the solvent, crystallisation was induced by adding a small amount of pentane, and gave dark-brown crystals (120 mg, 87%). M.p.: 205 °C (lit. 204 °C).[18b] MS (*m/z*): 277 $[M]^+$; ^{1}H NMR (CD_2Cl_2): $\delta =$ 9.38 (d, $J = 9.8$ Hz, 1H, $H_{(8)}$), 8.44 (d, $J = 9.3$ Hz, 1H, $H_{(4)}$), 8.35 (d, $J =$ 9.1 Hz, 2H, C_6H_4), 8.30 (d, $J = 4.7$ Hz, 1H, $H_{(2)}$), 8.06 (d, $J = 9.1$ Hz, 2H, C_6H_4), 7.88 (t, $J = 9.9$ Hz, 1H, $H_{(6)}$), 7.60 (t, $J = 9.7$ Hz, 1H, $H_{(5-7)}$), 7.49 (d, $J = 4.3$ Hz, 1H, $H_{(3)}$), 7.48 (t, $J = 9.6$ Hz, 1H, $H_{(5-7)}$); ^{13}C NMR ($CDCl_3$): $\delta =$ 157.8, 147.2, 145.3, 144.6, 140.7, 140.2, 139.0, 135.7, 128.2, 125.5, 124.8, 122.5, 121.3; $C_{16}H_{11}N_3O_2$: calcd C 69.31, H 4.00, N 15.15; found C 69.01, H 4.13, N 15.02.

X-ray crystallography: The data were collected on a Stoe Imaging Plate Diffraction System (IPDS) equipped with an Oxford cryosystems cooler device, with a tube power of 2 kW for **2b** and **3**, and 1.5 kW for **2c**. The crystal to detector distance was 80 mm. Owing to rather low μx values, 0.014, 0.016, and 0.027 for **2b**, **2c**, and **3**, respectively, no absorption corrections were considered. The structures were solved by direct methods (Shelxs-86)[42] and refined by least-square procedures. Crystallographic data for **2b**, **2c**, and **3** are summarized in Table 7. The weighting Scheme used in the last refinement cycles was $w = w'[1 - (\Delta F/6\sigma(F_o)^2]^2$ where $w' = 1/\Sigma_1^n A_r T_i(x)$ with 5 coefficients A_r for the Chebyshev polynomial $A_r T_r(x)$, where x was F_c/F_c(max). The calculations were carried out with the CRYSTALS package programs[43] running on a PC. The drawings of the molecular structures were obtained with the help of CAMERON.[43] The atomic scattering factors were taken from International Tables for X-ray Crystallography.[44]

Crystallographic data (excluding structure factors) for the structures reported in this paper have been deposited with the Cambridge Crystallographic Data Centre as supplementary publication no. CCDC-127823–127825. Copies of the data can be obtained free of charge on application to CCDC, 12 Union Road, Cambridge CB2 1EZ, UK (fax: (+44) 1223-336-033; e-mail: deposit@ccdc.cam.ac.uk).

Spectroscopy: The changes in dipole moment between ground and excited states ($\Delta\mu$) were obtained from solvatochromism through the Lippert–Mataga Equation (3).[45]

$$\tilde{\nu}_{CT} = \tilde{\nu}^g_{CT} + C_1(n^2-1)/(2n^2+1) + C_2[(D-1)/(D+2) - (n^2-1)/(n^2+2)] \quad (3)$$

where $\tilde{\nu}_{CT}$ is the frequency (cm^{-1}) of the optical transition in a particular solvent, $\tilde{\nu}^g_{CT}$ is the frequency in the gas phase, D and n are the dielectric constant and refraction index of the solvent, and C_1 and C_2 are constants. The constant C_2 can be determined from least-square fit of Equation (2) to the charge transfer band in different solvent and allows the determination of $\Delta\mu$ through Equation (4):

$$C_2 = 2\mu_g \Delta\mu / hca^3 \quad (4)$$

© WILEY-VCH Verlag GmbH, D-69451 Weinheim, 2000
0947-6539/00/0614-2606 $ 17.50+.50/0 *Chem. Eur. J.* **2000**, *6*, No. 14

Table 7. Crystal data collections and refinements.

	2b	**2c**	**3**
Crystal data			
chemical formula	$C_{16}H_{11}N_3O_2$	$C_{34}H_{28}N_4O_2$	$C_{32}H_{38}N_8O_7$
molecular weight	277.3	524.6	646.7
crystal system	monoclinic	monoclinic	triclinic
space group	*P*c	$P2_1/n$	$P\bar{1}$
a [Å]	6.4003(6)	15.999(2)	7.539(1)
b [Å]	3.7733(3)	6.318(1)	11.365(1)
c [Å]	26.454(3)	27.870(3)	19.358(3)
α [deg]			83.58(2)
β [deg]	95.79(1)	104.99(1)	83.77(2)
γ [deg]			73.81(1)
V [Å^3]	635.6	2722.6	1578.0
ρ(calcd) [g cm^{-3}]	1.45	1.28	1.36
$\mu(Mo_{K\alpha})$ [cm^{-1}]	0.917	0.75	0.919
crystal size [mm]	$0.32\times0.15\times0.07$	$0.15\times0.15\times0.40$	$0.37\times0.37\times0.17$
T [K]	160	160	140
Data collection			
radiation	$Mo_{K\alpha}$($\lambda=0.71069$ Å)	$Mo_{K\alpha}$	$Mo_{K\alpha}$
scan mode	ϕ	ϕ	ϕ
2θ range	$4.6<2\theta<48.4$	$4.5<2\theta<48.3$	$4<2\theta<48.4$
absorption correction	none	none	none
measured reflections	4131	13952	12972
independant reflections	1891	4754	4766
observed reflections	1616	2397	3127
criteria	$I>3\sigma(I)$	$I>2\sigma(I)$	$I>3\sigma(I)$
Refinement			
refinement on	*F*	*F*	*F*
R[a]	0.038	0.054	0.046
Rw[b]	0.044	0.053	0.053
no of parameters used	191	362	425
H atoms treatment	calculated	calculated	calculated
weighting scheme	Chebychev	Chebychev	Chebychev
coeff. ar	2.21	1.72	1.62
	−1.36	0.173	−0.739
	2.17	1.78	1.24
	−0.663	0.014	−0.477
	0.552	0.551	0.242
$\Delta\rho_{max}$ [e Å^{-3}]	0.93	0.83	0.59
$\Delta\rho_{min}$ [e Å^{-3}]	−0.83	−0.74	−0.23

[a] $R=\Sigma(||F_o|-|F_c||)/\Sigma(|F_o|)$. [b] $Rw=\Sigma w(|F_o|-|F_c|)^2/\Sigma w(F_o)^2]^{1/2}$.

where *h* and *c* are the Planck's constant and the speed of the light, respectively, and *a* is the Onsager radius, estimated to be equal to 4.7 Å and 5.5 Å (for **2b** and **3**, respectively) from the solute molar volume[46] and the crystal data available. However, the evaluation of $\Delta\mu$ by the Lippert–Mataga treatment rises several problems, which have been discussed in the literature.[47] Therefore, this approach may not be fully reliable.

NLO properties

Powder efficiencies: The measurements of second harmonic generation (SHG) intensity were carried out by the Kurtz–Perry powder technique,[48] using a picosecond Nd/YAG pulsed (10 Hz) laser operating at $\lambda=1.064$ μm. The outcoming Stokes-shifted radiation at 1.907 μm generated by Raman effect in a hydrogen cell (1 m long, 50 atm) was used as the fundamental beam for second harmonic generation. The SHG signal was selected through a suitable interference filter, detected by a photomultiplier and recorded on an ultrafast Tektronic TDS 620 B oscilloscope.

EFISH measurements: The principle of the electric field induced second harmonic (EFISH) technique is reported elsewhere.[20, 49] The data were recorded using the 1.907 μm incident laser beam generated as described above. The laser delivered pulses of 10 ns. The compounds were dissolved in dioxane at various concentrations (0 to 5×10^{-3} mol l^{-1}). The centrosymmetry of the solution was broken by dipolar orientation of the chromophores with a high voltage pulse (around 5 kV) synchronized with the laser pulse. The dipole moment were measured independently by a classical method based on the Guggenheim theory.[50] Further details of the experimental methodology and data analysis are reported elsewhere.[49]

Theoretical methods: The all-valence INDO (intermediate neglect of differencial overlap) method,[51] in connection with the sum-over-state (SOS) formalism,[52] was employed. Details of the computationally efficient INDO/SOS based method for describing second-order molecular optical nonlinearities have been reported elsewhere.[4] Calculation was performed using the INDO/1 Hamiltonian incorporated in the commercially available MSI software package INSIGHT II (4.0.0). The monoexcited configuration interaction (MECI) approximation was employed to describe the excited states. The 100 energy transitions between the ten highest occupied molecular orbitals and the ten lowest unoccupied ones were chosen to undergo CI mixing. Structural parameters used for the INDO calculations were taken from the present crystal study for **2b**, **2c** (molecule 1), and **3**.

Electrochemistry: Electrochemical measurements were carried out in an airtight three-electrodes cell connected to a vacuum argon/N_2 line, using the interrupt method to minimize the uncompensated resistance (iR) drop. Cyclic voltammetry was recorded in acetonitrile, with $Bu_4N^+BF_4^-$ as supporting electrolyte (0.1 M L^{-1}). The working electrode was platinum, and a saturated calomel electrode (SCE) was used as a reference. The scan rate was 100 mV s^{-1}. Electrolysis was performed at −1000 mV using platinum foil as a working electrode.

Acknowledgement

The authors deeply acknowledge Jean-François Delouis, Isabelle Fanton-Maltey and Olivier Guilbaud for their help in EFISH measurements, and Dr. de Montauzon for the electrochemical measurement.

[1] a) P. N. Prasad, D. J. Williams, *Introduction to Nonlinear Optical Effects in Molecules and Polymers*, Wiley, Chichester, **1991**; b) *Molecular Nonlinear Optics*: *Materials*, *Physics*, *and Devices* (Ed.: J. Zyss), Academic Press, New York, **1994**; c) *Nonlinear Optical Properties of Organic Materials VII*, *Vol. 2285* (Ed. G. R. Mohlmann), Proc. SPIE, The International Society for Optical Engineering: Washington, DC, **1994**.

[2] For recent reviews see: a) L. R. Dalton, A. W. Harper, R. Ghosn, W. H. Steier, M. Ziari, H. Fetterman, Y. Shi, R. V. Mustacich, A. K-Y. Jen, K. J. Shea, *Chem. Mater.* **1995**, *7*, 1060–1081; b) R. G. Benning, *J. Mater. Chem.* **1995**, *5*, 365–378; c) *Optical Nonlinearities in Chemistry* (Ed. D. M. Burland), *Chem. Rev.* **1994**, *94*, Issue 1; d) T. Verbiest, S. Houbrechts, M. Kauranen, K. Clays, A. Persoons, *J. Mater. Chem.* **1997**, *7*, 2175–2189; e) J. J. Wolff, R. Wortmann, *Adv. Phys. Org. Chem.* **1999**, *32*, 121–217.

[3] S. R. Marder, D. N. Beratan, L. T. Cheng, *Science* **1991**, *252*, 103 – 106.
[4] a) D. R. Kanis, T. J. Marks, M. A. Ratner, *Int. J. Quant. Chem.* **1992**, *43*, 61 – 82; b) D. R. Kanis, M. A. Ratner, T. J. Marks, *Chem. Rev.* **1994**, *94*, 195 – 242.
[5] a) L. T. Cheng, W. Tam, S. H. Stevenson, G. R. Meredith, G. Rikken, S. R. Marder, *J. Phys. Chem.* **1991**, *95*, 10631 – 10643; b) L. T. Cheng, W. Tam, S. R. Marder, A. E. Stiegman, G. Rikken, C. W. Spangler, *J. Phys. Chem.* **1991**, *95*, 10643 – 10652.
[6] V. Pushkana Rao, A. K.-Y. Jen, J. Chandrasekhar, I. N. Namboothiri, A. Rathna, *J. Am. Chem. Soc.* **1996**, *118*, 12443 – 12448.
[7] S. M. LeCours, H.-W. Guan, S. G. DiMagno, C. H. Wang, M. J. Therien, *J. Am. Chem. Soc.* **1996**, *118*, 1497 – 1503.
[8] M. Blanchard-Desce, V. Alain, P. V. Bedworth, S. R. Marder, A. Fort, C. Runser, M. Barzoukas, S. Lebus, R. Wortmann, *Chem. Eur. J.* **1997**, *3*, 1091 – 1104.
[9] H. J. Tobler, A. Bauder, H. H. Gunthard, *J. Mol. Spectrosc.* **1965**, 18, 239.
[10] K. P. Zeller, in *Houben Weyl*, *Methoden der Organischen Chemie*, *Vol. 5/2c*, Thieme, Stuttgart, **1985**, p. 127.
[11] S. Schmitt, M. Baumgarten, J. Simon, K. Hafner, *Angew. Chem.* **1998**, *110*, 1129 – 1133; *Angew. Chem. Int. Ed.* **1998**, *37*, 1078 – 1081.
[12] J. E. Frey, A. M. Andrews, S. D. Combs, S. P. Edens, J. J. Puckett, R. E. Seagle, L. A. Torreano, *J. Org. Chem.* **1992**, *57*, 6460 – 6466.
[13] S. Ito, S. Kikuchi, N. Morita, T. Asao, *Chem. Lett.* **1996**, 175 – 176.
[14] a) J. O. Morley, *J. Am. Chem. Soc.* **1988**, *110*, 7660 – 7663; b) J. O. Morley, *J. Chem. Soc. Perkin Trans. 2* **1989**, 103 – 106.
[15] A. E. Asato, R. S. H. Liu, V. Pushkara Rao, Y. M. Cai, *Tetrahedron Lett.* **1996**, *37*, 419 – 422.
[16] G. Iftime, P. G. Lacroix, K. Nakatani, A. C. Razus, *Tetrahedron Lett.* **1998**, *39*, 6853 – 6856.
[17] R. Hermann, B. Pedersen, G. Wagner, J.-H. Youn, *J. Organomet. Chem.* **1998**, *571*, 261 – 266.
[18] a) F. Gerson, E. Heilbronner, *Helv. Chim. Acta* **1958**, *41*, 1444 – 1463; b) F. Gerson, J. Schulze, E. Heilbronner, *Helv. Chim. Acta* **1958**, *41*, 1463 – 1481; c) A. G. Anderson, Jr., J. A. Nelson, J. J. Tazuma, *J. Am. Chem. Soc.* **1953**, *75*, 4980 – 4989.
[19] Among recent examples for the NLO use of DR1, see: a) D. H. Choi, J. H. Park, T. H. Rhee, N. Kim, S.-D. Lee, *Chem. Mater.* **1998**, *10*, 705 – 709; b) N. Tirelli, U. W. Suter, A. Altomare, R. Solaro, F. Ciardelli, S. Follonier, Ch. Bosshard, P. Günter, *Macromolecules* **1998**, *31*, 2152 – 2159; c) H. Jiang, A. K. Kakkar, *Macromolecules* **1998**, *31*, 2501 – 2508.
[20] For a general discussion of the EFISH technique, see: a) J. L. Oudar, *J. Chem. Phys.* **1977**, *67*, 446 – 457; b) B. F. Levine, C. G. Betha, *J. Chem. Phys.* **1975**, *63*, 2666 – 2682, B. F. Levine, C. G. Betha, *J. Chem. Phys.* **1976**, *65*, 1989 – 1993.
[21] a) J. O. Morley, V. J. Dorcherty, D. Pugh, *J. Chem. Soc. Perkin Trans. 2* **1987**, 1351 – 1355; b) J. O. Morley, *J. Chem. Soc. Faraday Trans. 2* **1991**, *87*, 3009 – 3013; c) J. O. Morley, *Int. J. Quantum Chem.* **1993**, *46*, 19 – 26; d) J. O. Morley, *J. Chem. Soc. Perkin Trans. 2* **1995**, 731 – 734.
[22] D. Li, M. A. Ratner, T. J. Marks, *J. Am. Chem. Soc.* **1988**, *110*, 1707 – 1715.
[23] P. A. Franken, A. E. Hill, C. W. Peters, G. Weinrich, *Phys. Rev. Lett.* **1961**, *7*, 118 – 119.
[24] Among early attempts to use DR1 in polymers for NLO purpose, see: K. D. Singer, J. E. Sohn, S. J. Lalama, *Appl. Phys. Lett.* **1986**, *49*, 248 – 250.
[25] D. J. Williams, *Angew. Chem.* **1984**, *96*, 637 – 650; *Angew. Chem. Int. Ed. Engl.* **1984**, *23*, 690 – 703.
[26] J. Zyss, J. L. Oudar, *Phys. Rev. A* **1982**, *26*, 2028 – 2048.
[27] On the correlation of dipole moment with acentric space groups, see: J. K. Whitesell, R. E. Davis, L. L. Saunders, R. J. Wilson, J. P. Feagins, *J. Am. Chem. Soc.* **1991**, *113*, 3267 – 3270.
[28] a) K. D. Singer, J. E. Sohn, L. A. King, H. M. Gordon, H. E. Katz, C. W. Dirk, *J. Opt. Soc. Am. B* **1989**, *6*, 1339 – 1350; b) F. Gerson, T. Gaumann, E. Heilbronner, *Helv. Chim. Acta* **1958**, *41*, 1481 – 1491.
[29] C. R. Moylan, R. J. Twieg, V. Y. Lee, S. A. Swanson, K. M. Betterton, R. D. Miller, *J. Am. Chem. Soc.* **1993**, *115*, 12599 – 12600.
[30] M. L. Glowka, Z. Olubek, *Acta Crystallogr. C* **1994**, *50*, 458 – 460, and references herein.
[31] J. L. Oudar, J. Chemla, *J. Chem. Phys.* **1977**, *66*, 2664 – 2668.
[32] See for example: a) V. Alain, S. Rédoglia, M. Blanchard-Desce, S. Lebus K. Lukaszuk, R. Wortmann, U. Gubler, C. Bosshard, P. Günter, *Chem. Phys.* **1999**, *245*, 51 – 71; b) M. Blanchard-Desce, V. Alain, L. Midrier, R. Wortmann, S. Lebus, C. Glania, P. Kramer, A. Fort, J. Muller, M. Barzoukas, *J. Photochem. Photobiol. A* **1997**, *105*, 115 – 121.
[33] See for example: a) D. R. Kanis, M. A. Ratner, T. J. Marks, *J. Am. Chem. Soc.* **1992**, *114*, 10338 – 10357; b) S. Di Bella, I. Fragalà, I. Ledoux, T. J. Marks, *J. Am. Chem. Soc.* **1995**, *117*, 9481 – 9485.
[34] J. L. Oudar, J. Zyss, *Phys. Rev. A* **1982**, *26*, 2016 – 2027.
[35] B. F. Levine, C. G. Bethea, C. D. Thurmond, R. T. Lynch, J. L. Bernstein, *J. Appl. Phys.* **1979**, *50*, 2523 – 2527.
[36] J. Zyss, D. S. Chemla, J. F. Nicoud, *J. Chem. Phys.* **1981**, *74*, 4800 – 4811.
[37] S. Di Bella, I. Fragalà, T. J. Marks, M. A. Ratner, *J. Am. Chem. Soc.* **1996**, *118*, 12747 – 12751.
[38] a) R. Yam, R. Cohen, G. Berkovic, *Nonlinear Opt.* **1995**, *11*, 311; b) P. M. Lundquist, S. Yitzchaik, T. J. Marks, G. K. Wong, S. Di Bella, R. Cohen, G. Berkovic, *Phys. Rev. B* **1997**, *55*, 14055 – 14058.
[39] I. Malfant, N. Cordente, P. G. Lacroix, C. Lepetit, *Chem. Mater.* **1998**, *10*, 4079 – 4087.
[40] B. Bosnich, *J. Am. Chem. Soc.* **1968**, *90*, 627 – 632.
[41] A. A. S. Briquet, H.-J. Hansen, *Helv. Chim. Acta* **1994**, *77*, 1577 – 1584.
[42] G. M. Sheldrick, *SHELXS86*, *Program for Crystal Structure Solution*, University of Göttingen, Göttingen, Germany, **1986**.
[43] a) D. J. Watkin, C. K. Prout, J. R. Carruthers, P. W. Betteridge, *CRYSTALS Issue 10*, Chemical Crystallography Laboratory, University of Oxford, Oxford, **1996**; b) D. J. Watkin, C. K. Prout, L. J. Pearce, *CAMERON*, Chemical Crystallography Laboratory, University of Oxford, Oxford, **1996**.
[44] D. T. Cromer, J. T. Waber, *International Tables for X-ray Crystallography*, *Vol. 4*, Kynoch Press, Birmingham, **1974**.
[45] N. Mataga, T. Kubota, *Molecular Interactions and Electronic Spectra*, Marcel Dekker, New York, **1970**, p. 371.
[46] S. Di Bella, T. J. Marks, M. A. Ratner, *J. Am. Chem. Soc.* **1994**, *116*, 4440 – 4445.
[47] W. Liptay, *Z. Naturforschg.* **1965**, *20a*, 1441 – 1471.
[48] a) S. K. Kurtz, T. T. Perry, *J. Appl. Phys.* **1968**, *39*, 3798 – 3813; b) J. P. Dougherty, S. K. Kurtz, *J. Appl. Crystallogr.* **1976**, *9*, 145 – 158.
[49] I. Maltey, J. A. Delaire, K. Nakatani, P. Wang, X. Shi, S Wu, *Adv. Mater. Opt. Electronics* **1996**, *6*, 233 – 238.
[50] E. A. Guggenheim, *Trans. Faraday Soc.* **1949**, *45*, 714 – 720.
[51] a) M. C. Zerner, G. Loew, R. Kirchner, U. Mueller-Westerhoff, *J. Am. Chem. Soc.* **1980**, *102*, 589 – 599; b) W. P. Anderson, D. Edwards, M. C. Zerner, *Inorg. Chem.* **1986**, *25*, 2728 – 2732.
[52] J. F. Ward, *Rev. Mod. Phys.* **1965**, *37*, 1 – 18.

Received: August 25, 1999
Revised version: November 26, 1999 [F2002]

 © WILEY-VCH Verlag GmbH, D-69451 Weinheim, 2000 0947-6539/00/0614-2608 $ 17.50+.50/0